 Human Molecular Genetics, 2002, Vol. 11, No. 25 3221–3229

A full-coverage, high-resolution human chromosome 22 genomic microarray for clinical and research applications

Patrick G. Buckley[1,‡], Kiran K. Mantripragada[1,‡], Magdalena Benetkiewicz[1], Isabel Tapia-Páez[2], Teresita Diaz de Ståhl[1], Magnus Rosenquist[1], Haider Ali[1], Caroline Jarbo[1], Cecilía de Bustos[1], Carina Hirvelä[1], Birgitta Sinder Wilén[1], Ingegerd Fransson[2], Charlotte Thyr[1], Britt-Inger Johnsson[1], Carl E.G. Bruder[1,†], Uwe Menzel[1], Martin Hergersberg[3], Nils Mandahl[4], Elisabeth Blennow[2], Anna Wedell[2], David M. Beare[5], John E. Collins[5], Ian Dunham[5], Donna Albertson[6], Daniel Pinkel[6], Boris C. Bastian[6], A. Fawad Faruqi[7], Roger S. Lasken[7], Koichi Ichimura[8], V. Peter Collins[8] and Jan P. Dumanski[1,*]

[1]Department of Genetics and Pathology, Rudbeck laboratory, Uppsala University, 751 85 Uppsala, Sweden, [2]Department of Molecular Medicine, CMM building, Karolinska Hospital, 171 76 Stockholm, Sweden, [3]Zentrum für Labormedizin, Kantonsspital Aarau, CH-5001 Aarau, Switzerland, [4]Department of Clinical Genetics, Lund University Hospital, Lund, Sweden, [5]The Wellcome Trust Sanger Institute, Wellcome Trust Genome Campus, Hinxton, Cambridge, CB10 1SA, UK, [6]UCSF Comprehensive Cancer Center, Box 0808, University of California, San Francisco, CA 94143-0128, USA, [7]Molecular Staging, Inc., 300 George Street, 7th Floor, New Haven, CT 06511, USA and [8]Department of Pathology, Division of Molecular Histopathology, University of Cambridge, Addenbrooke's Hospital, Hills Road, Cambridge CB2 2QQ, UK

Received August 20, 2002; Revised and Accepted October 1, 2002

We have constructed the first comprehensive microarray representing a human chromosome for analysis of DNA copy number variation. This chromosome 22 array covers 34.7 Mb, representing 1.1% of the genome, with an average resolution of 75 kb. To demonstrate the utility of the array, we have applied it to profile acral melanoma, dermatofibrosarcoma, DiGeorge syndrome and neurofibromatosis 2. We accurately diagnosed homozygous/heterozygous deletions, amplifications/gains, *IGLV/IGLC* locus instability, and breakpoints of an imbalanced translocation. We further identified the 14-3-3 eta isoform as a candidate tumor suppressor in glioblastoma. Two significant methodological advances in array construction were also developed and validated. These include a strictly sequence defined, repeat-free, and non-redundant strategy for array preparation. This approach allows an increase in array resolution and analysis of any locus; disregarding common repeats, genomic clone availability and sequence redundancy. In addition, we report that the application of phi29 DNA polymerase is advantageous in microarray preparation. A broad spectrum of issues in medical research and diagnostics can be approached using the array. This well annotated and gene-rich autosome contains numerous uncharacterized disease genes. It is therefore crucial to associate these genes to specific 22q-related conditions and this array will be instrumental towards this goal. Furthermore, comprehensive epigenetic profiling of 22q-located genes and high-resolution analysis of replication timing across the entire chromosome can be studied using our array.

INTRODUCTION

Chromosome 22 is the second smallest human chromosome and has been a testing ground for recent genomic advances allowing fundamental biological questions to be approached from a global perspective. It contains ~600 genes, which represent 2.4% of all known genes. The first comprehensive

*To whom correspondence should be addressed at: Department of Genetics and Pathology, Rudbeck laboratory 3rd floor, Uppsala University, Dag Hammarskjölds väg 20, 751 85 Uppsala, Sweden. Fax: +46 18558931; Email: jan.dumanski@genpat.uu.se
†Present address: AstraZenenca R&D, Transgenics and Comparative Genomics, 43183 Mölndal, Sweden.
‡The authors wish it to be known that, in their opinion, these two authors should be considered as joint First Authors.

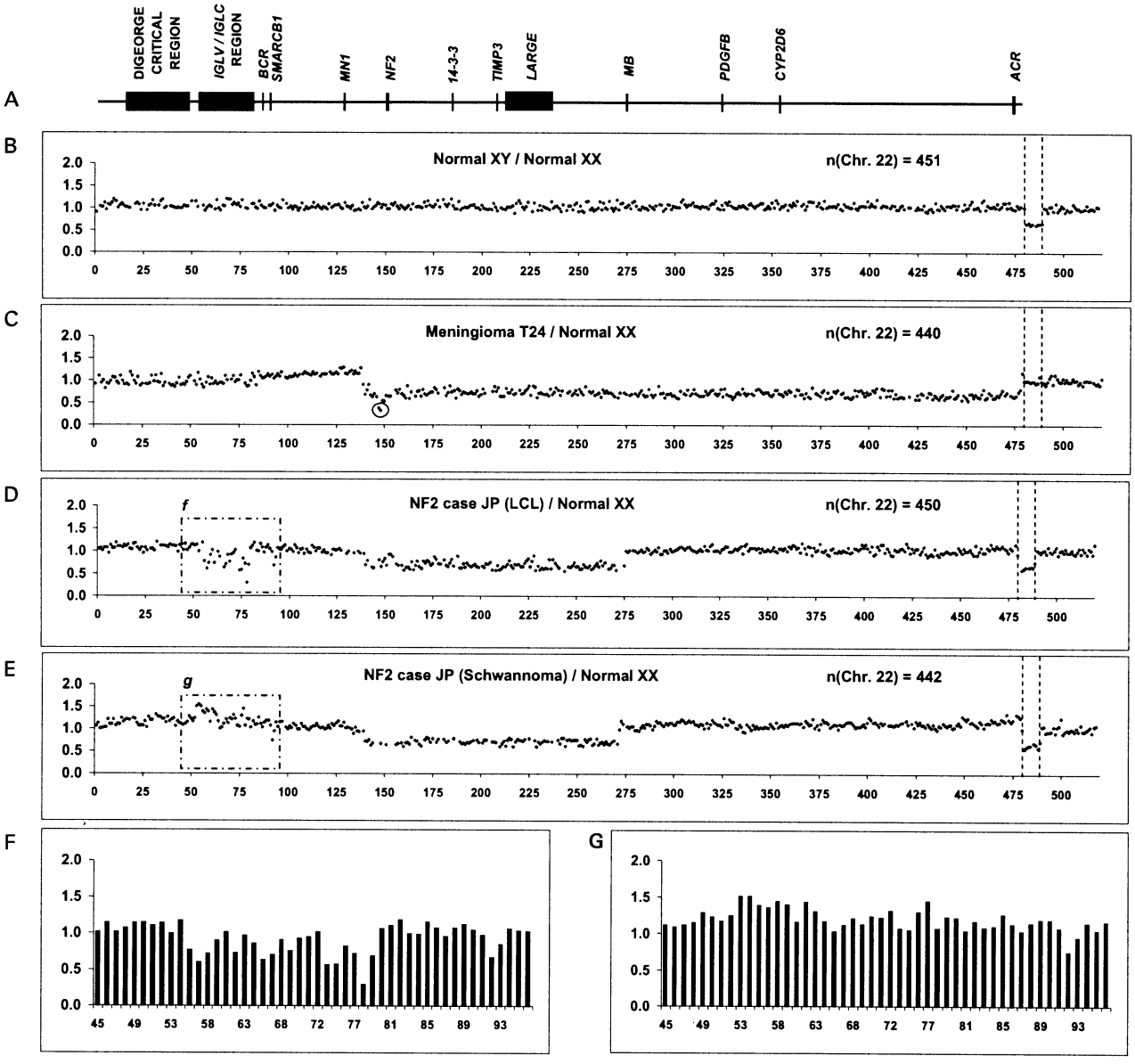

Figure 1. Validation of the chromosome 22 array. (**A**) Schematic map of selected genes and disease-related regions from chromosome 22, drawn to scale according to their positions on the minimal tiling path. We defined a region of ID12–47 and ID52–80 on the array, as the DiGeorge Critical Region (DGCR) and *IGLV*/*IGLC* region, respectively (18,33). (**B**–**E**) Display 4 array-CGH experiments of the entire array, which contains a total of 520 loci. The X-axis displays 480 chromosome 22 loci, ordered from centromere (left hand side) to telomere (right hand side). Dots between the vertical broken lines indicate control loci from chromosome X (9 clones). Dots plotted after the chromosome X controls are derived from chromosomes other than X and 22 (31 clones). The n(Chr. 22)-value denotes the number of 22q loci that were scored in a single experiment. Each dot on a chart represents the normalized, average ratio between fluorescent signals for each locus (Y-axis), which are derived from 3–4 independent replica spots on the array, in a single hybridization experiment. (B) Normalized average ratio from hybridization of normal male (XY) versus normal female (XX) DNA. (C) Normalized average ratio from experiment using meningioma T24 tumor DNA derived from a female patient versus normal female DNA (9). Circle outlines two consecutive loci (ID147 and 148, normalized average ratio 0.37 and 0.32, respectively), which are deleted homozygously in this tumor. Panel (D) and (E) show the results from two experiments using DNA derived from LCL of NF2 case JP and the schwannoma tumor DNA, derived from the same patient (9,10,34). (**F** and **G**) Enlarged, detailed normalized CGH profile of *IGLV*/*IGLC* loci, which are derived from experiments showed in panels (D) and (E) respectively. Loci ID54, 62, 65 and 73 were excluded from analysis due insufficient quality of data in both experiments.

linkage map over chromosome 22 was constructed in 1991, the complete YAC-based physical map was established in 1995, and, in 1999, it was the first sequenced chromosome (1–3). Microarray-based comparative genomic hybridization (array-CGH) is rapidly emerging as a powerful tool for a variety of genetic applications (4,5), particularly as it provides significant advantages over conventional techniques for detection of gene dosage alterations. A genome-wide scanning array, with an average resolution of 1.3 Mb, has recently been published (6). We have constructed and tested the first high-resolution chromosomal genomic microarray, which will allow the study of disease genes and other research questions related to this

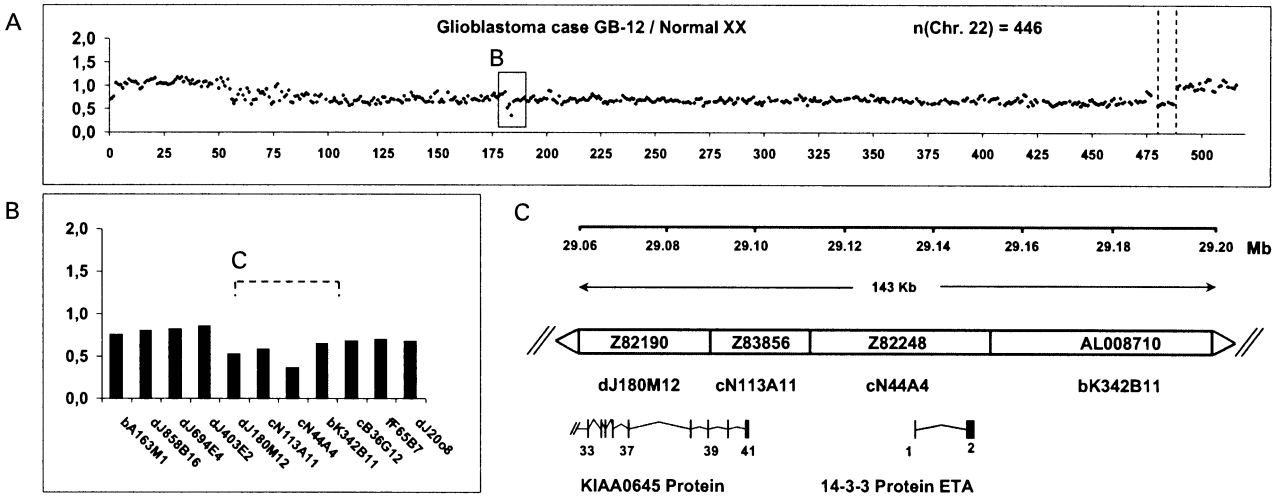

Figure 2. Detection of a novel, homozygous deletion in glioblastoma case GB-12 from a male patient. (**A**) The general layout follows the structure described for Figure 1. Both copies of chromosome 22, situated between the peri-centromeric region and locus ID55, are retained in the tumor. The large terminal deletion encompasses ID56–480. The homozygously deleted single cosmid (locus ID186, clone cN44A4, acc. no. Z82248) displayed a normalized CGH ratio of 0.35. (**B**) Enlarged, normalized CGH profile of 11 loci centered around the homozygous deletion. (**C**) Detailed transcriptional map of 4 genomic clones located in the vicinity of cosmid cN44A4. Scale in Mb is according to Ensembl database. The gene encoding the 14-3-3 eta isoform (acc. Q04917) is entirely contained within cosmid cN44A4. Exon numbers are indicated beneath each transcript.

autosome. Use of the genomic DNA clones across the entire long arm of chromosome 22 provides both long-range coverage of 34.7 Mb and an exceptional average resolution of 75 kb.

RESULTS

Preparation of the array

We aimed to fully cover known segments of chromosome 22q with genomic clones from the minimal tiling path (3) without gaps larger than 100 kb. Therefore, we selected a set of 460 loci derived from chromosome 22, together with nine X chromosome loci and 31 loci from other chromosomes, as controls. There are 167 cosmids/fosmids and 329 BACs/PACs on the array. Four loci were covered using a novel, repeat-free, non-redundant PCR-based strategy (Table 1; described below). In addition, 20 clones were amplified in parallel using phi29 DNA polymerase and represented as independent measurement points (http://puffer.genpat.uu.se/chrom_22_array/chrom22.htm). Each locus has an ID number, with the chromosome 22 loci assigned numbers 1–480 (including phi29 amplified clones), ordered from centromere to telomere. The chromosome 22 part of the array spans 34.7 Mb, which results in an average resolution of 75 kb. The array contains a 161 kb gap (0.46% of 34.7 Mb, on the telomeric side of ID323, acc. AL022318), which was due to the failure in confirming the correct identity of one clone, using our quality control criteria (http://puffer.genpat.uu.se/chrom_22_array/chrom22.htm). Other regions not represented on the array were excluded based on bioinformatic analysis (see Materials and Methods), which clearly indicated that these sequences are unsuitable for CGH analysis. All clones within these intervals were found to contain high repeat content (up to 99%) and/or stretches of strong sequence similarity (spanning $\geq$15 kb with overall sequence identity of $\geq$98%) to other human chromosomes and/or other regions on 22q. For instance, the pericentromeric region showed strong similarities to chromosome 14, which is in agreement with recent analysis of segmental duplications in the genome (7). Thus, these chromosome 22 loci are practically unapproachable by current methods.

Validation of the array

To evaluate the chromosome 22 array for detection of copy number variation we carried out a series of experiments, four of which are shown in Figure 1. In the normal XY/normal XX hybridization (Fig. 1B), all chromosome 22 loci and control loci from other autosomes showed 2 copies (*A*verage *N*ormalized *I*nter-*L*ocus *F*luorescence *R*atio: ANILFR; 1.03 ± 0.07), while chromosome X controls provided a sensitive means to detect 1 copy (ANILFR 0.64 ± 0.018). Meningioma T24 is a previously reported tumor with homozygous and heterozygous deletions (8,9). Hence, it allows detection of zero, one and two copies of loci across chromosome 22 (Fig. 1C). In addition to the homozygous deletion (ID147 and 148, ANILFR 0.34 ± 0.03), we also observed the large terminal heterozygous deletion (ANILFR 0.70 ± 0.06).

The neurofibromatosis type 2 (NF2) case JP (constitutional DNA derived from lymphoblastoid cell line; LCL) is another well characterized patient with a 6 Mb heterozygous interstitial deletion (9,10). We detected this deletion between ID140–275 (ANILFR 0.67 ± 0.07; Fig. 1D). We also observed a region of genomic instability within the immunoglobulin lambda variable and constant chain loci (*IGLV*/*IGLC*). This region (Fig. 1D and F) displayed a single homozygous deletion in ID78 (normalized fluorescent ratio 0.28) surrounded by at least 3 pockets of heterozygously deleted loci. To verify this finding, we examined schwannoma DNA from the same patient (Fig. 1E) and confirmed the presence of the 6 Mb

heterozygous deletion (ANILFR 0.7 ± 0.05). In contrast, the *IGLV*/*IGLC* region exhibited a shift towards gain in copy number (Fig. 1G). Figure 1F and G highlights the differences in behavior of the *IGLV*/*IGLC* region in LCL and tumor material from the same patient. Color switch experiments were performed for all the above described samples confirming these results (not shown).

Research applications of chromosome 22 array

Chromosome 22 contains several uncharacterized disease-causing genes. For instance, previous low-resolution loss-of-heterozygosity studies of glioblastoma indicated that chromosome 22 harbors a tumor suppressor gene(s), implicated in development of this aggressive and incurable tumor (11,12). We applied the array to profile two previously studied glioblastomas (GB-12 and GB-28) (unpublished). Array-CGH confirms the presence of large heterozygous deletions in both cases. Unexpectedly, we also detected a homozygous deletion of ID186 (cosmid cN44A4) in case GB-12 (Fig. 2). This observation was confirmed by Southern analysis using probes derived from this locus (not shown). The non-zero value for the ratio in the homozygously deleted region may be due to a normal tissue component in the tumor, inefficient blocking of repetitive sequences, autofluorescence of the target clones or that cosmid cN44A4 is larger than the deletion. Cosmid cN44A4 contains a single gene encoding the 14-3-3 protein eta isoform (acc. Q04917). The 14-3-3 eta is a member of a protein family, which are known regulators of mitosis, apoptosis and various signal transduction pathways (13,14). It is relevant to point out that the 14-3-3-sigma isoform has recently been implicated as a tumor suppressor in breast cancer (15,16). From the functional point of view, the 14-3-3 eta gene is a plausible candidate tumor suppressor gene. However, it should be noted that two neighboring clones on the centromeric side (cosmid cN113A11 and PAC dJ180M12, Fig. 2B) also show reduced fluorescent ratios. Thus, other genes located in the vicinity of this locus, for example, the novel gene KIAA0645 with no assigned function, should also be further studied. This hypothesis should be corroborated by analysis of this locus in a larger series of glioblastomas.

Another type of tumor studied was acral melanoma, which is a rare form of cutaneous melanoma that does not seem to be related to UV-exposure (17). Previous metaphase-CGH showed that acral melanomas differed from other melanomas by amplifications/gains involving regions on 11q13, 22q11–13 and 5p15 (17). Fifteen acral melanomas were hybridized and 8 samples showed different patterns of amplifications/gains, with respect to their regional distribution along 22q and level of copy number variation. Three profiles are shown in Figure 3. We also confirmed the previous report of 5p15 gains (17), as a number of control loci from chromosome 5p15 revealed gains in AM-12 (Fig. 3A) and other tumors (not shown). Thus, analysis of a larger series of acral melanomas, at the same resolution across the whole genome, is likely to reveal new information and might elucidate mechanisms underlying tumorigenesis of these tumors.

The chromosome 22 array as a diagnostic tool

We employed the array as a diagnostic tool in several well studied disorders, such as NF2, DiGeorge syndrome and dermatofibrosarcoma protuberans (DFSP) (Fig. 4). Using peripheral blood DNA from a female NF2 patient p41, with a moderate disease phenotype, we detected and sized a large heterozygous deletion. The deletion covered ID132–177 (~3.3 Mb), which included the *NF2* gene (ID151–156) (Fig. 4A). This is a rare example of an NF2 patient with an interstitial deletion extending far towards the centromere from the *NF2* gene (9,10).

We applied this array in the analysis of previously characterized DiGeorge patients with deletions in the DiGeorge Critical Region (DGCR) (unpublished). One of these subjects (DNA derived from LCL of DG16_01) is shown in Figure 4B. As expected, the deletion spans the region between Low Copy Repeats A–D (18), which are located in ID16–47 (2.4 Mb). This demonstrates the usefulness of the array in the diagnosis of DiGeorge syndrome. However, array-CGH results are difficult to interpret for some loci within DGCR. Bioinformatic analysis of these loci provides clues to their unexpected behavior. For instance, a majority of clones are cosmids with a high content of common repeats (>50%). We therefore assume that the deletion is contiguous. The difficulties in analysis of DGCR are also in agreement with reports of segmental duplications on 22q (3,7). These results demonstrate the need for an array specifically tailored for analysis of DGCR. In summary, in all experiments with DiGeorge patients at least 14 clones within the DGCR are reliable for diagnosis of disease-causing deletions.

The array has further been applied in the analysis of dermatofibrosarcoma protuberans (DFSP). DFSP is a cutaneous tumor, the cytogenetic features of which include the translocation t(17;22)(q22;q13) or, more commonly, supernumerary ring chromosomes containing material from 17q and 22q (19,20). Previous studies revealed that these rearrangements result in a fusion between collagen type I, alpha 1 gene (*COL1A1*) from chromosome 17 and the platelet derived growth factor, B-chain gene (*PDGFB*) from chromosome 22. Array-CGH was carried out on two DFSPs (TNM2 and T843; Fig. 4C and D). These tumors contain the *COL1A1*/*PDGFB* fusion gene (21,22) and in both cases we detected the breakpoint at ID325 (Fig. 4C–F). This clone contains the entire *PDGFB* gene, which is truncated as a consequence of the translocation (Fig. 4F). Strikingly, the 22q loci which follow after ID325 towards the telomere (ID326–480) behave as if they were affected by a terminal, heterozygous deletion. The ANILFR for these clones in both experiments are at the level of chromosome X controls (Fig. 4C and D). We also observed a low level gain in both tumors, involving the 22q segment centromeric to the translocation breakpoint, which is in agreement with previous cytogenetic reports (23). Both tumors were studied cytogenetically and were found to have a diploid nature, except for chromosomes 17 and 22 (22). Thus, non-22 autosomal controls in array-CGH confirm the diploid nature of these tumors and allow proper normalization of CGH results. Another finding, seen in both tumors, was the presence of several independent peaks of amplification at an even higher level (Fig. 4C and D), which is compatible with the genetic instability of ring chromosomes (24).

Developments of array-CGH methodology

We experimented with a novel, strictly sequence-defined and PCR-based strategy for preparation of gene dosage arrays

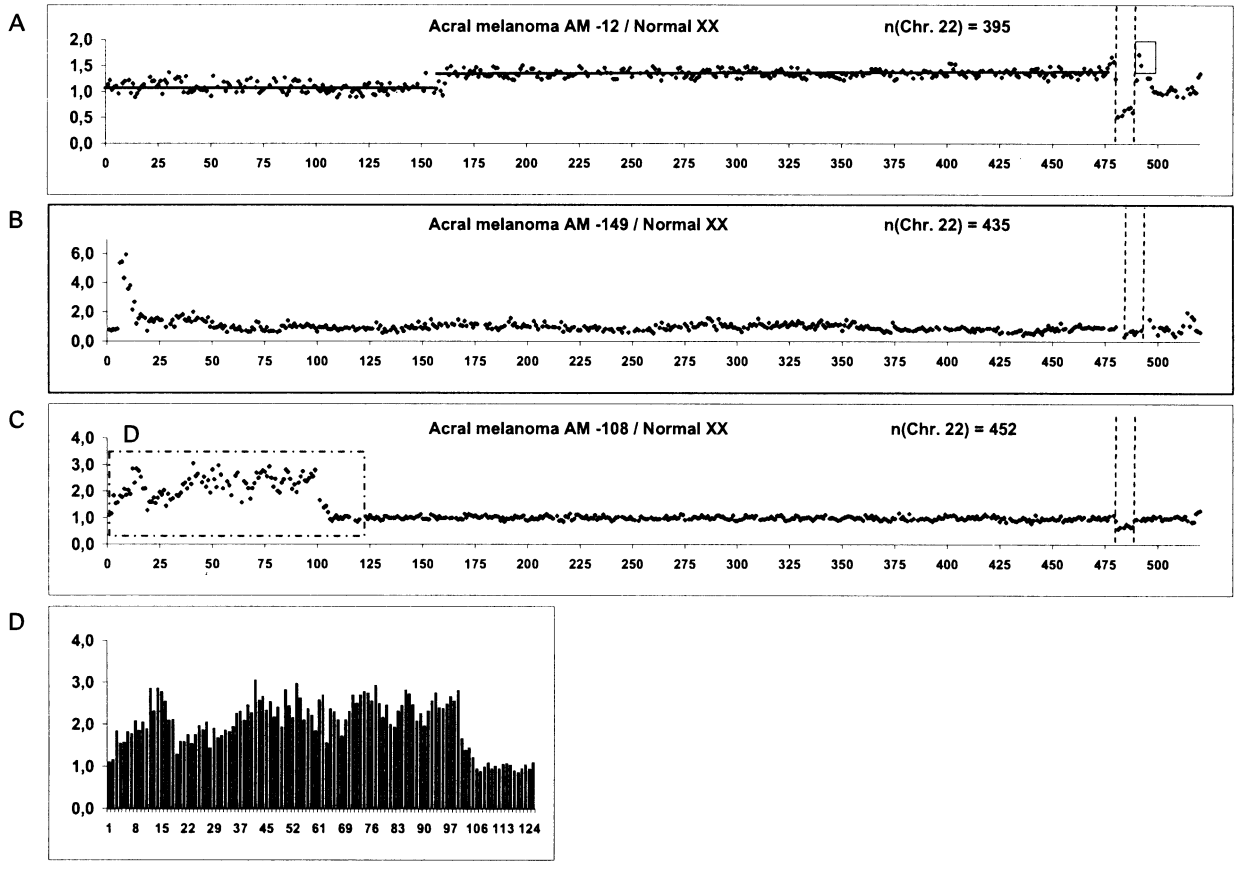

Figure 3. Chromosome 22 array-CGH profile of DNA from 3 male acral melanomas, versus normal female DNA. The general layout follows the structure described for Figure 1. (**A**) Partial gain of 22q in tumor AM-12 from locus ID162 to the telomere. Two horizontal trend lines are introduced to highlight the shift in the level of copy number. The normalized ratio of fluorescent signals in the amplified region is ~1.5, which indicates an average of 3 copies. The rectangle denotes reproducible gains of loci on chromosome 5, which were excluded from normalization. Two highest ratios were observed for ID491 and 492, normalized fluorescence ratio of 1.7 and 1.5, respectively. (**B**) Amplification of a region in the vicinity of the centromere in tumor AM-149. The amplicon is composed of 8 clones (ID6–13), with the highest normalized ratio of fluorescence at 5.9 for ID9, which indicates ~12 copies. (**C**) Gain of ID3–104 in tumor AM-108. (**D**) Enlarged view of the amplified region in tumor AM–108. The highest ratio of fluorescence reaches a level of 3 (ID14, 41, 53, 77, 85, 99; fluorescence ratio of 2.8, 3.0, 2.9, 2.9, 2.8 and 2.8, respectively), which is consistent with up to 6 copies for these loci.

Table 1. Chromosome 22 loci analyzed using the repeat-free, PCR-based procedure for preparation of the array

Locus ID	Replaced genomic clone (clone name/acc. no.)	Average repeat content (%)	Size of the gap (kb)	No. of PCR fragments/ average size (bp)	Size range of PCR fragments (bp)	Total length of PCR fragments (kb)	Primer modification
107	BAC RP11-89B2/AL080245	48.0	63	47/495	302–913	23.282	5′ amino
108	BAC CTA-125H2/Z98949	41.8	174	45/592	296–887	26.671	5′ amino
268	PAC RP1-272J12/Z82194	50.5	161	39/744	549–1133	29.017	Unmodified
393	YAC PRYR7CC1/AL049760	50.6	119	47/529	245–951	24.862	5′ amino

(patent pending) (25), using pools of non-redundant DNA fragments in four 22q loci (Table 1). The rationale was to test an approach, which would overcome limitations of array-CGH for regions covered by genomic clones with a high repeat content or containing duplications of sequence in the human genome. Results from all experiments described in this paper fully confirm that the pools perform as reliable replacements for genomic clones. Two of these experiments are shown in Figure 5. Furthermore, there was no detectable difference in the results obtained from unmodified primers, as compared to DNA amplified using 5′-amino-labeled oligonucleotides (Table 1).

The other successful development was the application of phi29 DNA polymerase in the preparation of DNA, prior to printing of the array. One of the main constraints of standard array-CGH protocols is a low yield of DNA obtained from PACs and BACs. This often requires costly repetitions of large-scale preparations. The goal was to test the performance of DNA amplified with phi29 polymerase. Phi29 DNA polymerase is a highly processive, proof-reading and strand displacing DNA polymerase derived from the phi29 phage of *Bacillus subtilis.* Large linear and circular DNA molecules can be efficiently amplified using the rolling circle amplification principle.

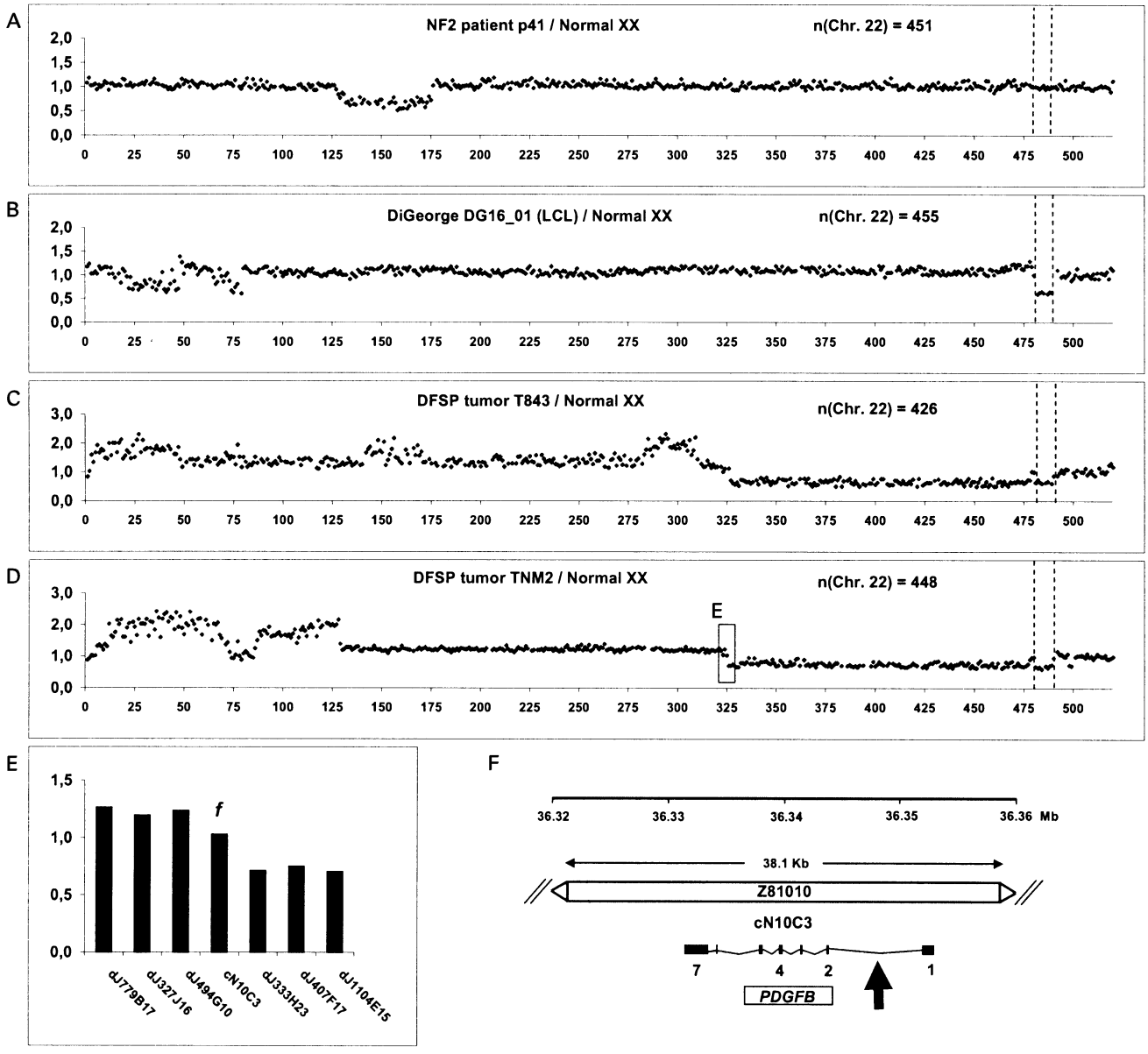

Figure 4. Diagnostic applications of the chromosome 22 array in the analysis of constitutional and tumor-associated aberrations. The general layout follows the structure described for Figure 1. (**A**) CGH profile of female NF2 patient, showing a large constitutional heterozygous deletion of ID132–177, encompassing the *NF2* gene. (**B**) Analysis of constitutional heterozygous deletions in a male patient affected with DiGeorge syndrome. The deletion within DGCR extends from ID16–47 (2.4 Mb). This case displayed 14 clones, which were clearly heterozygously deleted (IDs 16, 22, 25, 27, 28, 29, 33, 36, 37, 39, 41, 44, 46 and 47; ANILFR 0.70 ± 0.04). Increase of fluorescence ratio was observed for a number of loci within the deleted interval and this could be explained by high content of common repeats (see results). Note that the instability of the *IGLV*/*IGLC* region is also evident in this experiment (see above Fig. 1 and results). (**C** and **D**) Analysis of dermatofibrosarcoma protuberans (DFSP) tumor DNA from two male patients T843 and TNM2. The region of chromosome 22 covered by ID326-480 in (C) and (D) shows identical results for both tumors. The fluorescence ratio of these loci is at the level observed for X controls, which is consistent with 1 copy of this region. Tumor TNM2 showed a large, low level gain region (ID129–322, ANILFR 1.23 ± 0.06). Also for T843, the ANILFR within one discontinuous segment of 22q was uniform (ID48–140 ANILFR 1.35 ± 0.10 and ID171–280 ANILFR 1.36 ± 0.10). (**E**) Enlarged view of fluorescence ratio for clones in the vicinity of cosmid cN10C3 from analysis of tumor TNM2. (**F**) Detailed view of the *PDGFB* locus drawn to scale with regard to gene size and genomic length of insert from cosmid cN10C3. The vertical arrow indicates the position of the breakpoint between chromosome 17 and 22, located within intron 1 of the *PDGFB* gene. Exon numbers are indicated beneath the *PDGFB* transcript.

Exponential amplification yields are obtained using exonuclease resistant random hexamers in an overnight isothermal reaction (26,27). Twenty clones (http://puffer.genpat.uu.se/chrom_22_array/chrom22.htm/phi29_amplified_clones) were processed in two ways: *i*) using standard Qiagen-based protocols; and *ii*) using 10 ng of DNA derived from Qiagen preparation as template. Approximately 50 µg of DNA was produced in a single overnight phi29-reaction, which will suffice for the production of >6000 microarrays. The phi29 amplified DNA was quality controlled as described in the Materials and

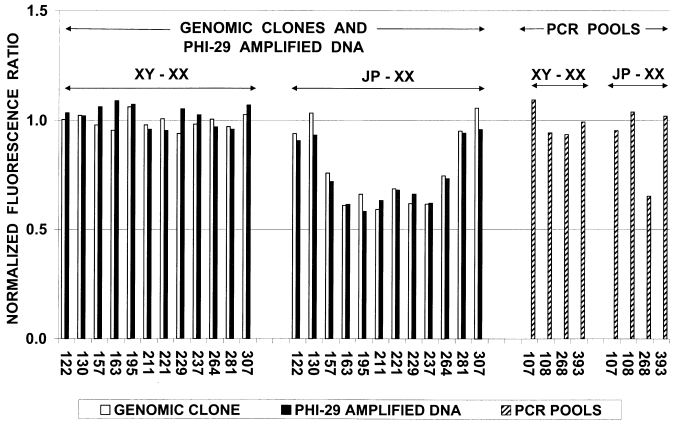

Figure 5. Chromosome 22 loci amplified using phi29-polymerase and PCR-based repeat-free strategies. Comparison of array-CGH results for DNA from 12 genomic clones, amplified with phi29 DNA polymerase and prepared using standard methods (ID122, 130, 157, 163, 195, 211, 221, 229, 237, 264, 281 and 307), are shown on the left hand side. Results from hybridization to 4 PCR pools (ID107, 108, 268 and 393) are displayed on the right hand side. The outcome of two independent experiments is compiled; CGH of normal male (XY) with normal female (XX), and hybridization of NF2 case JP (LCL, containing 6 Mb constitutional heterozygous deletion, encompassing ID: 157, 163, 195, 211, 221, 229, 237, 264 and 268) with normal female (XX).

Methods. The results of phi29 amplified DNA from two array-CGH experiments are described in Figure 5. We also compared data from additional hybridizations for the 20 loci (not shown). In summary, the phi29 polymerase-based protocol performs well and is a reliable way to produce DNA for array-CGH.

DISCUSSION

Reliable and high-resolution measurement of copy number variation is fundamental in diagnostics and many areas of genetic research. This array is the first in a new generation of high-resolution genetic tools. We provide 95% coverage across 34.7 Mb (1.1% of the human genome) with unprecedented average resolution of ~75 kb. Several examples shown in this study highlight the power and future potential of this array.

Chromosome 22 array in the research and molecular diagnosis of disease

DFSP is a rare and locally aggressive tumor, which is sometimes misdiagnosed as dermatofibroma, a common and benign lesion (28,29). This leads to inadequate primary treatment and high recurrence rate, which is up to 50% overall, but 13–20% after adequate excision (28,29). Better diagnostic tools would therefore improve treatment. All previously studied cases of DFSP, displayed a presence of the *COL1A1*/*PDGFB* fusion gene, which offers the possibility to develop diagnostic tools (22). We show here that our array offers a quick molecular diagnostic kit, based on detection of the breakpoint for imbalanced translocation on 22q in combination with loss of genetic material, distal to the breakpoint. This is the first report of array-CGH in detection of imbalanced translocation breakpoints, which has a diagnostic value.

Detection of ~40 kb homozygous deletion in GB12, while scanning 34 Mb of 22q in glioblastoma, is an illustrative example of the sensitivity and comprehensiveness of our analysis. It is also a strong indication that investigation of a larger tumor series with this degree of resolution will reveal a highly complex picture of aberrations occurring in this type of cancer. It should also be stressed here that the segment encompassing the 14-3-3 eta-isoform gene is not located within the primary glioblastoma candidate region on 22q. It was previously positioned closer to the telomere of 22q, using the low resolution LOH/microsatellite-based genotyping (11,12).

We observed a genetic instability in the *IGLV*/*IGLC* region, which was most pronounced in DNA from LCLs derived from EBV-transformed B-lymphocytes. EBV-carrying LCLs are polyclonal after transformation, oligoclonal on prolonged *in vitro* culturing, eventually becoming monoclonal (30). The LCL from NF2 case JP displayed heterozygous and homozygous deletions within *IGLV*/*IGLC* (Fig. 1D). The other studied LCLs displayed heterozygous deletions or no detectable aberrations in this locus. Deletions within *IGLV*/*IGLC* can be explained, due to rearrangements of the immunoglobulin loci during B-cell maturation. A more detailed analysis of LCLs at different stages of *in vitro* culturing should be carried out. Results from the schwannoma of NF2 case JP, when compared with the analysis of LCL from the same patient (Fig. 1D and E), suggests that the *IGLV*/*IGLC* locus displays a general genetic instability, which is not restricted to B-lymphocytes. Another even more important implication of the above results is that this array, at the current level of resolution across the entire 22q, provides an opportunity to study the possible presence of deletion/amplification polymorphisms in human DNA samples derived from normal, non-related, multi-ethnic populations.

Future strategies for array construction and applications of the array

Chromosome 22 is a suitable experimental platform for developing new technologies in array-CGH. It is a challenging subject as the tiling path of 22q is rich in inter- and intra-chromosomal segmental duplications (also denoted as Low Copy Repeats), common repeats and pseudogenes (3,7), which restrict the analysis of this important chromosome. Current protocols for array-CGH rely on human Cot-1 DNA for suppression of background derived from common repeats. However, Cot-1 DNA is expensive and the quality of different commercially available batches is extremely variable. Thus, a decrease in the amount of Cot-1 DNA, or its full elimination from array-CGH is desirable. Additional drawbacks associated with genomic clones include their unavailability, contamination with bacteriophages, inserts that are prone to rearrangements and purchasing of expensive clones from private distributors. Our repeat-free strategy eliminates a majority of the above limitations and would permit analysis of any locus in the human and other sequenced genomes. The above reasoning and difficulties encountered in diagnosing DiGeorge-associated deletions, highlight a need for a second generation, higher resolution array, which is entirely based on the repeat-free strategy. It should be further stressed that the repeat-free strategy also allows for a significant increase in array-CGH

resolution, currently down to a 20 kb genomic segment (in preparation). A further considerable improvement of the methodology is the application of phi29 polymerase in preparation of ready-to-print DNA that entails a considerable advantage with regard to work input.

A wide range of questions in basic research and diagnostics may now be approached using our array. These include comprehensive epigenetic profiling of 22q-located genes and high-resolution analysis of replication timing across the entire chromosome. Moreover, chromosome 22 contains a considerable number of uncharacterized disease genes, e.g. familial schizophrenia susceptibility, glioblastoma and other types of astrocytoma, ependymoma, meningioma, schwannomatosis, pheochromocytoma, breast and colon cancer (31). As chromosome 22 is well characterized with regard to active gene content, it is therefore critical to link the known genes to the above mentioned conditions. Our high resolution array will be instrumental towards this goal.

MATERIALS AND METHODS

Selection and preparation of genomic target clones

We used the tiling path of clones derived from the effort towards sequencing of chromosome 22 (3) (www.ensembl.org). The identity of each clone was verified and quality controlled by agarose gel electrophoresis of native/*Eco*RI-digested DNA and STS-PCR using at least one marker for each clone. DNA from Qiagen preparations was quantified using picoGreen assay (Molecular Probes, Inc., Eugene, OR).

Preparation of the PCR pools

The genomic sequences were downloaded from NCBI (www.ncbi.nlm.nih.gov). The common repeats were masked using *RepeatMasker* (ftp.genome.washington.edu/RM/) and the 'masked' output file was analysed by *blastn* against the *nr*-section of the EMBL database. Further, we used the Oligo6 program to design primers in the non-redundant regions. Standard protocols were employed for amplification of DNA using total human DNA as template. The size of amplified fragments was controlled and quantification was carried out by picoGreen assay (Molecular Probes, Inc.). All fragments from a single locus were pooled, prior to dissolving in printing solution. Detailed information can be found at: http://puffer.genpat.uu.se/chrom_22_array/chrom22.htm.

Amplification of DNA by phi29 polymerase

DNA from genomic clones (10 ng) was placed into a 96-well plate in a total volume of 100 µl containing 37 mM Tris–HCl, pH 7.5, 50 mM KCl, 10 mM $MgCl_2$, 5 mM $(NH_4)_2SO_4$, 1.0 mM dNTPs, 50 µM exonuclease-resistant hexamer, 1 unit/ml of yeast pyrophosphatase (Roche Molecular Biochemicals, Indianapolis IN) and 800 units/ml phi29 DNA polymerase (Amersham Biosciences, Piscataway NJ; Templiphi DNA Sequencing Template Amplification kit, catalogue no. 25-6400-10). Reactions were incubated for 16 h at 30°C and terminated by heating to 65°C for 3 min in a PCR System Thermocycler (Applied Biosystems, Foster City, CA) (27).

Printing of the array, hybridizations, scanning and image analysis

Methods used for array production, DNA labeling, hybridization and post-hybridization processing are shown at: http://puffer.genpat.uu.se/chrom_22_array/chrom22.htm. DNA was sonicated, precipitated and dissolved in 80% DMSO. DNA was printed on aminosilane-coated slides using the ProSys robot (Cartesian Technologies, Irvine, CA) and 12 SMP3 pins (TeleChem International, Sunnyvale, CA), with a center-to-center distance of 250 µm between adjacent spots. Each clone was printed in quadruplicate. One microgram of test and reference DNA was labeled by random priming with CY3 dCTP (PA 53021, Amersham Biosciences) and CY5 dCTP (NEN Life Science Products, Boston, MA), respectively, followed by hybridization (9,32). Image acquisition was performed using the GenePix 4000B scanner (Axon Instruments Inc, Union City, CA). Analysis of hybridization intensity was carried out using the GenePixPro image analysis software (Axon Instruments). Ratio of the intensities between test DNA and reference DNA was calculated using 'the ratio of means' formula. The GenePixPro software subtracts the local background from the signal intensities for each spot. The average, standard deviation and co-efficient of variance of the four replicas for each clone were also calculated. Clones displaying a co-efficient of variance greater than 5% between a minimum of three replica-spots were discarded from further analysis (unsuccessfully scored loci). The average ratio from the non-chromosome 22 autosomal controls was used in the normalization of all average ratio values from all clones on the array, in each hybridization experiment.

The ANILFR values were calculated in order to assess the inter-locus variation, representing a region(s) on the array. The normalized ratio for successfully scored loci from a certain, continuous region on the array was used to calculate the ANILFR value and standard deviation.

ACKNOWLEDGEMENTS

We thank Dr Bruce A Roe and the staff of the Advanced Center for Genome Technology, University of Oklahoma, for providing chromosome 22 genomic clones. We would also like to thank Drs Rolf Ohlsson, Ulf Landegren, Maria Kost-Alimova, Stephan Imreh, Ulf G. Pettersson, Kenneth Nilsson, Monika Nister and Göran Levan for critical review of the manuscript. This work was supported by grants from the U.S. Army Medical Research and Materiel Command, award no. DAMD17-00-1-0536, the Swedish Cancer Foundation, the Swedish Research Council and Uppsala University to J.P.D. C.D.B is supported by a fellowship from the Department of Education, Universities and Research of the Basque Government for the formation of researchers. I.D., J.E.C. and D.M.B. are supported by the Wellcome Trust.

REFERENCES

1. Dumanski, J.P., Carlbom, E., Collins, V.P., Nordenskjöld, M., Emanuel, B.S., Budarf, M.L., McDermid, H., Wolff, R., O'Connell, P., White, R. *et al.* (1991) A map of 22 loci on human chromosome 22. *Genomics*, **11**, 709–719.
2. Collins, J.E., Cole, C.G., Smink, L.J., Garrett, C.L., Leversha, M.A., Soderlund, C.A., Maslen, G.L., Everett, L.A., Rice, K.M., Coffey, A.J. *et al.* (1995) A high resolution integrated yeast artificial chromosome clone map of human chromosome 22. *Nature*, **377**, 367–379.
3. Dunham, I., Shimizu, N., Roe, B.A., Chissoe, S., Hunt, A.R., Collins, J.E., Bruskiewich, R., Beare, D.M., Clamp, M., Smink, L.J. *et al.* (1999) The DNA sequence of human chromosome 22. *Nature*, **402**, 489–495.
4. Solinas-Toldo, S., Lampel, S., Stilgenbauer, S., Nickolenko, J., Benner, A., Dohner, H., Cremer, T. and Lichter, P. (1997) Matrix-based comparative genomic hybridization: biochips to screen for genomic imbalances. *Genes Chromosomes Cancer*, **20**, 399–407.
5. Pinkel, D., Segraves, R., Sudar, D., Clark, S., Poole, I., Kowbel, D., Collins, C., Kuo, W.L., Chen, C., Zhai, Y. *et al.* (1998) High resolution analysis of DNA copy number variation using comparative genomic hybridization to microarrays. *Nat. Genet.*, **20**, 207–211.
6. Snijders, A.M., Nowak, N., Segraves, R., Blackwood, S., Brown, N., Conroy, J., Hamilton, G., Hindle, A.K., Huey, B., Kimura, K. *et al.* (2001) Assembly of microarrays for genome-wide measurement of DNA copy number. *Nat. Genet.*, **29**, 263–264.
7. Bailey, J.A., Yavor, A.M., Viggiano, L., Misceo, D., Horvath, J.E., Archidiacono, N., Schwartz, S., Rocchi, M. and Eichler, E.E. (2002) Human-specific duplication and mosaic transcripts: the recent paralogous structure of chromosome 22. *Am. J. Hum. Genet.*, **70**, 83–100.
8. Peyrard, M., Fransson, I., Xie, Y.-G., Han, F.-Y., Ruttledge, M.H., Swahn, S., Collins, J.E., Dunham, I., Collins, V.P. and Dumanski, J.P. (1994) Characterization of a new member of the human b-adaptin gene family from chromosome 22q12, a candidate meningioma gene. *Hum. Mol. Genet.*, **3**, 1393–1399.
9. Bruder, C.E., Hirvela, C., Tapia-Paez, I., Fransson, I., Segraves, R., Hamilton, G., Zhang, X.X., Evans, D.G., Wallace, A.J., Baser, M.E. *et al.* (2001) High resolution deletion analysis of constitutional DNA from neurofibromatosis type 2 (NF2) patients using microarray-CGH. *Hum. Mol. Genet.*, **10**, 271–282.
10. Bruder, C.E., Ichimura, K., Blennow, E., Ikeuchi, T., Yamaguchi, T., Yuasa, Y., Collins, V.P. and Dumanski, J.P. (1999) Severe phenotype of neurofibromatosis type 2 in a patient with a 7.4 MB constitutional deletion on chromosome 22: possible localization of a neurofibromatosis type 2 modifier gene? *Genes Chromosomes Cancer*, **25**, 184–190.
11. Ino, Y., Silver, J.S., Blazejewski, L., Nishikawa, R., Matsutani, M., von Deimling, A. and Louis, D.N. (1999) Common regions of deletion on chromosome 22q12.3–q13.1 and 22q13.2 in human astrocytomas appear related to malignancy grade. *J. Neuropathol. Exp. Neurol.*, **58**, 881–885.
12. Oskam, N.T., Bijleveld, E.H. and Hulsebos, T.J. (2000) A region of common deletion in 22q13.3 in human glioma associated with astrocytoma progression. *Int. J. Cancer*, **85**, 336–339.
13. Fu, H., Subramanian, R.R. and Masters, S.C. (2000) 14-3-3 proteins: structure, function, and regulation. *Annu. Rev. Pharmacol. Toxicol.*, **40**, 617–647.
14. Yaffe, M.B. (2002) How do 14-3-3 proteins work? Gatekeeper phosphorylation and the molecular anvil hypothesis. *FEBS Lett.*, **513**, 53–57.
15. Vercoutter-Edouart, A.S., Lemoine, J., Le Bourhis, X., Louis, H., Boilly, B., Nurcombe, V., Revillion, F., Peyrat, J.P. and Hondermarck, H. (2001) Proteomic analysis reveals that 14-3-3sigma is down-regulated in human breast cancer cells. *Cancer Res.*, **61**, 76–80.
16. Umbricht, C.B., Evron, E., Gabrielson, E., Ferguson, A., Marks, J. and Sukumar, S. (2001) Hypermethylation of 14-3-3 sigma (stratifin) is an early event in breast cancer. *Oncogene*, **20**, 3348–3353.
17. Bastian, B.C., Kashani-Sabet, M., Hamm, H., Godfrey, T., Moore, D.H., 2nd, Brocker, E.B., LeBoit, P.E. and Pinkel, D. (2000) Gene amplifications characterize acral melanoma and permit the detection of occult tumor cells in the surrounding skin. *Cancer Res.*, **60**, 1968–1973.
18. Shaikh, T.H., Kurahashi, H., Saitta, S.C., O'Hare, A.M., Hu, P., Roe, B.A., Driscoll, D.A., McDonald-McGinn, D.M., Zackai, E.H., Budarf, M.L. *et al.* (2000) Chromosome 22-specific low copy repeats and the 22q11.2 deletion syndrome: genomic organization and deletion endpoint analysis. *Hum. Mol. Genet.*, **9**, 489–501.
19. Pedeutour, F., Simon, M.P., Minoletti, F., Barcelo, G., Terrier-Lacombe, M.J., Combemale, P., Sozzi, G., Ayraud, N. and Turc-Carel, C. (1996) Translocation t(17;22) (q22;q13) in dermatofibrosarcoma protuberans. A new tumor-associated chromosome rearrangement. *Cytogenet. Cell Genet.*, **72**, 171–174.
20. Nishio, J., Iwasaki, H., Ishiguro, M., Ohjimi, Y., Yo, S., Isayama, T., Naito, M. and Kikuchi, M. (2001) Supernumerary ring chromosome in a Bednar tumor (pigmented dermatofibrosarcoma protuberans) is composed of interspersed sequences from chromosomes 17 and 22: a fluorescence in situ hybridization and comparative genomic hybridization analysis. *Genes Chromosomes Cancer*, **30**, 305–309.
21. Simon, M.P., Pedeutour, F., Sirvent, N., Grosgeorge, J., Minoletti, F., Coindre, J.M., Terrier-Lacombe, M.J., Mandahl, N., Craver, R.D., Blin, N. *et al.* (1997) Deregulation of the platelet-derived growth factor B-chain gene via fusion with collagen gene COL1A1 in dermatofibrosarcoma protuberans and giant-cell fibroblastoma. *Nat. Genet.*, **15**, 95–98.
22. O'Brien, K.P., Seroussi, E., Dal Cin, P., Sciot, R., Mandahl, N., Fletcher, J.A., Turc-Carel, C. and Dumanski, J.P. (1998) Various regions within the alpha-helical domain of the COL1A1 gene are fused to the second exon of the PDGFB gene in dermatofibrosarcomas and giant-cell fibroblastomas. *Genes Chromosomes Cancer*, **23**, 187–193.
23. Pedeutour, F., Simon, M.-P., Minoletti, F., Sozzi, G., Pierotti, M.A., Hecht, F. and Turc-Carel, C. (1995) Ring chromosomes in dermatofibrosarcoma protuberans are low-level amplifiers of chromosome 17 and 22 sequences. *Cancer Res.*, **55**, 2400–2403.
24. Gisselsson, D., Hoglund, M., Mertens, F., Johansson, B., Dal Cin, P., Van den Berghe, H., Earnshaw, W.C., Mitelman, F. and Mandahl, N. (1999) The structure and dynamics of ring chromosomes in human neoplastic and non-neoplastic cells. *Hum. Genet.*, **104**, 315–325.
25. Dumanski, J.P. (2002) Gene dosage arrays, their production and use thereof, Swedish patent application, no. SE0200865-4. Sweden.
26. Dean, F.B., Nelson, J.R., Giesler, T.L. and Lasken, R.S. (2001) Rapid amplification of plasmid and phage DNA using Phi 29 DNA polymerase and multiply-primed rolling circle amplification. *Genome Res.*, **11**, 1095–1099.
27. Dean, F.B., Hosono, S., Fang, L., Wu, X., Faruqi, A.F., Bray-Ward, P., Sun, Z., Zong, Q., Du, Y., Du, J. *et al.* (2002) Comprehensive human genome amplification using multiple displacement amplification. *Proc. Natl Acad. Sci. USA*, **99**, 5261–5266.
28. Rutgers, E.J., Kroon, B.B., Albus-Lutter, C.E. and Gortzak, E. (1992) Dermatofibrosarcoma protuberans: treatment and prognosis. *Eur. J. Surg. Oncol.*, **18**, 241–248.
29. Fish, F.S. (1996) Soft tissue sarcomas in dermatology. *Dermatologic Surgery*, **22**, 268–273.
30. Nilsson, K. (1979) The nature of lymphoid cell lines and their relationship to the virus. In Epstein, M. and Achong, B. (eds.), *The Epstein-Barr Virus.* Springer-Verlag, New York, pp. 227–266.
31. Dumanski, J.P. (1996) The human chromosome 22-located genes and malignancies of the central nervous system. *Neuropathol. Appl. Neurobiol.*, **22**, 412–417.
32. Feinberg, A.P. and Vogelstein, B. (1984) A technique for radiolabelling DNA restriction endonuclease fragments to high specific activity. Addendum. *Anal. Biochem.*, **137**, 266–267.
33. Scambler, P.J. (2000) The 22q11 deletion syndromes. *Hum. Mol. Genet.*, **9**, 2421–2426.
34. Bruder, C.E., Ichimura, K., Tingby, O., Hirakawa, K., Komatsuzaki, A., Tamura, A., Yuasa, Y., Collins, V.P. and Dumanski, J.P. (1999) A group of schwannomas with interstitial deletions on 22q located outside the NF2 locus shows no detectable mutations in the *NF2* gene. *Hum. Genet.*, **104**, 418–424.